ARTICLE

GM-CSF-Loaded Nanoparticles for Photothermal-Assisted Immunotherapy against Orthotopic Bladder Cancer

Weifeng Ren[1,2,#], Xiaomeng Cai[2,3,#], Jun Chen[2,3,#], Lifo Ruan[2,3], Huiru Lu[2], Jiayu Zhang[2,3], Yi Hu[2,3,*] and Jimin Gao[1,*]

[1]Zhejiang Provincial Key Laboratory for Technology & Application of Model Organisms, School of Laboratory Medicine and Life Science, Wenzhou Medical University, Wenzhou, 325035, China

[2]CAS Key Laboratory for Biomedical Effects of Nanomaterials and Nanosafety, Institute of High Energy Physics, Chinese Academy of Sciences (CAS), Beijing, 100049, China

[3]University of Chinese Academy of Sciences, Beijing, 100049, China

*Corresponding Authors: Yi Hu. Email: huyi@ihep.ac.cn; Jimin Gao. Email: jimingao64@163.com

#The authors contributed equally to this study

ABSTRACT

This study reported the construction of GM-CSF-loaded chitosan/graphene oxide nanoparticles for photothermal therapy-assisted immunotherapy against murine orthotopic bladder cancer. The encapsulated GM-CSF in chitosan/graphene oxide nanoparticles facilitated their immobilization on biotinylated mouse orthotopic bladder cancer surface, resulting in slow release of antitumor immune adjuvant. Locally released GM-CSF efficiently recruited dendritic cells to bladder tumor sites, thereby promoting immune responses in mice. Thus, the activated immune response in mice provided enhanced antitumor effects. Meanwhile, the thermal effect from the nanoparticles upon light irradiation induced a significant increase in dendritic cells and T cells compared with other groups, which confirmed that the focal photothermal effect potentiated antitumor immune response to tumors.

1 Introduction

Despite tremendous efforts devoted to developing various strategies for cancer treatment, the overall mortality of cancer remains at a high rate [1]. Increasing attention has been paid to develop adjuvant-based immunotherapy as an alternative treatment modality to improve the therapeutic outcomes and prognosis [2–6]. In this therapeutic fashion, the cytotoxic T lymphocytes (CTLs) are recruited to suppress tumor cells, which arises from the exposure of tumor antigen to the immune system [7]. In the meantime, the metastases of tumor cells can be suppressed [8]. Hence, adjuvant-based immunotherapy provides a potential strategy for treating tumors in a safe and durable manner [9].

The tumor cells hold tumor-associated antigens and may trigger an immune response [10]. Nevertheless, tumor cells often exhibit inadequate antitumor immune responses due to the insufficient capacity to activate naive T cells for antigen processing and presentation [11]. Therefore, researchers have introduced

immunomodulatory molecules as cytokine adjuvants to re-program the tumor immunosuppressive microenvironment for augmenting the immune response. For example, in Phase I clinical trial, researchers have adopted granulocyte-macrophage colony-stimulating factor (GM-CSF) to boost the recruitment and proliferation of dendritic cells (DC) [12,13]. However, the complexity of the immune response process compromises its effectiveness [14,15]. Meanwhile, it needs to extend the treatment course of cytokine transfection, making it unsuitable for advanced patients [16]. Therefore, it is very challenging to develop a facile delivery approach to improve the effect of adjuvant-based immunotherapy.

Photothermal therapy emerges as a minimally invasive cancer treatment modality [17–19]. A large variety of nanomaterials [20–24], such as gold nanoparticles [25–27], carbon nanotubes [21–23,28], and nanographene (GO) [29–32], can efficiently convert optical energy into thermal energy serving for photothermal therapy. On the one hand, photothermal ablation of tumor cells enables the release of tumor antigens into the tumor tissue, triggering specific antitumor immunity [33]. On the other hand, hyperthermia generated by nanoparticles can significantly impact the physiological properties of tumor tissues, including enhancing tumor permeability, alleviating hypoxia, and reducing interstitial fluid pressure [34–39]. Of particular note, hypothermia-induced tumor cell death results in the release of tumor-associated antigens/neoantigens and, most importantly, the release of danger-associated molecular patterns, such as heat shock proteins, calreticulin, high-mobility group box proteins, etc., which further activates antigen-presenting cells (APCs)/DCs [40]. The integration of indocyanine green (ICG)-based photothermal therapy with *N*-dihydro-galacto-chitosan as an immune adjuvant has been developed as a cancer vaccine, and its therapeutic effect has been confirmed in preclinical studies [17,28].

For treatment of urothelial carcinoma of the bladder, one of the most dangerous urological malignancies [41], intravesical GM-CSF instillations have proven to be efficient [42]. The duration of GM-CSF exposure is critical for responses to intravesical therapy. Due to the unique physiological structure of the bladder, the instilled adjuvant is easily expelled with urine and bladder endothelial cell shedding, and the adjuvant is rapidly degraded. The ineffective maintenance of the drug concentration essentially reduces the therapeutic efficiency. Therefore, extended retention of adjuvant in bladder cancer lesions is demanded to reduce the number of doses, mechanical damage, and pain. A previous study in our laboratory found that streptavidin-mouse-derived GM-CSF (SA-mGM-CSF) infusion to the biotin-decorated superficial orthotopic bladder cancer in mice exhibited sound anti-tumor effects [43]. The wide application of nanotechnology in the pharmaceutical field has afforded a new horizon for improving the bioavailability and efficacy of drugs [44–49]. Combined with the abovementioned immunotherapy and photothermal therapy, we hypothesize that the nanosystem may integrate them to enhance the tumor treatment outcomes.

In this study, we sought to construct chitosan/GO nanoparticles encapsulating GM-CSF for photothermal effect-enhanced immunotherapy against orthotopic murine bladder cancer. We hypothesized that chitosan/GO hybrid nanoparticles could exert a photothermally destructive effect on the tumor, which releases a large amount of tumor-associated antigens and acts as an immune adjuvant to boost recruitment of DCs and generation of antitumor cytokines significantly. Furthermore, chitosan-coated GO can encapsulate and immobilize SA-mGM-CSF onto tumor tissues, thereby promoting the local immune responses. The nanoparticles-generated hyperthermia effect would further induce recruitment and maturation of DCs, resulting in enhanced infiltration of effective T cells. The nanoparticle-mediated photothermal-assisted immunotherapy exhibits more potent innate and adaptive immune responses than individual therapy, leading to synergistic anticancer effects against the tumors.

2 Materials and Methods

2.1 Reagents and Materials

All chemicals were purchased from Inno-Chem Co., Ltd. (Beijing, China) and used without further purification unless otherwise mentioned. Chitosan (CS, Mn = 5000) was obtained from Yuhuan Biomedical

Company (China) and used as obtained. Dialysis tube (Cutoff = 3.5 kDa or 7 kDa) and syringe filters were purchased from Sigma-Aldrich. Deionized water processed by Millipore Milli-Q was used in all the experiments.

RPMI 1640 medium and fetal bovine serum (FBS) were purchased from Gibco Company (USA). The 3-(4, 5-dimethyl thiazolyl-2)-2, 5-diphenyl tetrazolium bromide (MTT) was purchased from Solarbio (Beijing, China). SA-GM-CSFs were synthesized in our laboratory according to the established protocol [50]. Anti-mouse-CD8a PE, anti-mouse-CD80 FITC, anti-mouse-CD86 PE, anti-mouse-CD4 APC, anti-mouse-CD11c FITC, and antimouse-CD11b APC were purchased from eBioscience (USA).

2.2 Cells and Mouse Model

The MB49 cell line was obtained as a gift from Dr. I. C. Summerhayes of Lahey Clinic (Burlington, MA, USA). MB49 cells were cultivated in RPMI 1640 medium complemented with FBS (10%, v/v), penicillin/streptomycin (100 U/mL), and 0.1% sodium pyruvate. C57BL/6 mice were obtained from the Slack Laboratory Animal Center (Shanghai, China). A humidified incubator at 37°C and 5% CO_2 was used for cell culture. All animal experiments were carried out following institutional ethics committee regulations and guidelines for animal welfare (Wenzhou Medical University Animal Care and Use). An orthotopic murine model of bladder cancer was constructed by implanting 1×10^6 MB49 cells (100 mL of RPMI 1640 medium without FBS) into the bladder of mice. Mice were sedated with isoflurane, and the vaccine was injected subcutaneously.

2.3 Preparation and Characterization of Nanoparticles

CS/GO hybrid nanoparticles were constructed following the established method. Briefly, 50 mg of CS and 10 mg of EDTA were mixed in 9 mL of distilled water, and then 1 mL of sodium cholate wrapped GO solution was added. The mixture was ultrasonicated for 2 min. Then, 10 mL of ethanol was added dropwise to the system under vigorous stirring. Then, 30 μL of glutaraldehyde solution (25%) was added to the CS/GO nanoparticles solution and stirred for 4 h at room temperature. Extensive dialysis against distilled water removed EDTA and ethanol. Pure CS nanoparticles were constructed in a similar way without GO. GM-CSF proteins-encapsulated nanoparticles were prepared by mixing the CS/GO nanoparticles with GM-CSF solution under agitation overnight. The GM-CSF@CS/GO nanoparticles were obtained by centrifugation at 12 krpm for 30 min, and the precipitation was dispersed in PBS buffer for further use. The amount of unbound protein in the supernatant was analyzed by UV-Vis spectroscopy.

2.4 Bioactivity Assays of SA-mGM-CSF

We used flow cytometric analysis and bone marrow cell proliferation assays to examine the biotin-SA interactions and GM-CSF bioactivity of the SA-GM-CSF. To prepare biotin-decorated cells, we firstly incubated 5×10^7 MB49 cells in PBS containing 1.0 mg/mL EZ-Link NHS-PEG4-Biotin (Pierce) for 1 h at room temperature. After thorough rinsing of the biotinylated cells with PBS, 0.1 mg/mL SA-mGM-CSF was added and incubated at room temperature. After one hour, the modified cells were washed thoroughly with PBS and stained with a phaeochrome-conjugated anti-GM-CSF monoclonal antibody (BD Biosciences) for 1 h at 37°C. The anchoring efficiency of the protein on the cell surface was determined by the flow cytometer (Becton Dickinson, San Jose, CA, USA). GM-CSF bioactivity of SA-mGM-CSF was assessed by myeloid cell proliferation. Briefly, bone marrow cells were collected from the femur and tibia of C57BL/6 mice by rinsing the bone marrow cavity. The obtained cells were transferred into 96-well plates at a density of 1×10^4 cells per well. These cells were stimulated with or without the indicated concentrations of SA-mGM-CSF fusion protein or recombinant mouse GM-CSF and further cultured for 3 days at 37°C in a humidified 5% CO_2 incubator. Subsequently, 20 μL of 5 mg/mL MTT solution was added to each well and incubated for 4 h. 200 μL of dimethyl sulfoxide was next added to each well, and its UV-vis absorbance of 570 nm was measured.

2.5 Intravesical Immobilization of SA-mGM-CSF and SA-mGM-CSF-Loaded Nanoparticles

An MB49 orthotopic murine model of bladder cancer was established to assess the feasibility and efficacy of immunotherapy by *in-situ* anchoring of SA-mGM-CSF or nanoparticles encapsulating SA-mGM-CSF on the bladder. Briefly, female C57BL/6 mice (8- to 10-week-old, 15–20 g) were anesthetized with intraperitoneal injections of sodium pentobarbital (68 mg/kg body weight). Then, we inserted a 24-gauge Insyte IV catheter (BD Biosciences) into the murine bladder through the urethra. To implant the tumor cells, chemical damage to the bladder mucosal surface was caused by the exposure with acid (0.1 M HCl, 15 s), followed by neutralization with base (0.1 M NaOH, 5 s). The contents were flushed with PBS *via* urethral infusion. Afterward, 1×10^6 MB49 cells were perfused into the bladder and incubated for 1 h. After one day, NHS-PEG4-biotin was perfused into the bladder and incubated for 1 h before rinsing by PBS. Then, the solution of PBS, SA-mGM-CSF, SA-mGM-CSF@CS, and SA-mGM-CSF@CS/GO (The dose of SA-mGM-CSF was 0.75 mg/kg) were instilled into bladder and allowed for incubation for two hours. After washing by PBS, the bladders were irradiated with NIR (808 nm, 0.35 W, 15 min). During irradiation, the temperature of the lesion was monitored by using a thermal infrared thermometer. The treatment was carried out two times per week for a total of three times. During the therapeutic period, the body temperature, food consumption, haematuria, and tumor palpability of mice were monitored. Also, the body weight of mice was monitored every other day.

2.6 Therapeutic Study

On the 15th day after the injection of immunoadjuvant, the bladders of tumor-bearing mice in each treatment group were sampled. The weight of the bladder was then measured, and photographs of the bladder were taken. Histological sections of the bladder, and other organs were stained with hematoxylin and eosin.

2.7 Analysis of Immune Cells

The proportion of T lymphocytes in the blood and the bladder was studied using FCM. Bladders were first collected from tumor-bearing mice and pressed into single-cell suspensions with a syringe plunger. After rinsing with PBS twice, cells were stained with anti-mouse-CD4 APC, anti-mouse-CD8a PE, anti-mouse-CD80 FITC, anti-mouse-CD86 PE, anti-mouse-CD11c FITC, and anti-mouse-CD11b APC for 30 min at 4°C according to the manufacturer instructions. After washing and filtering by a nylon filter membrane, the cell samples were analyzed by FCM through FL 1, FL 2, FL 3, and FL 4 channels.

2.8 Statistical Analysis

Unless otherwise stated, all data are expressed as mean ± standard deviation. One-way ANOVA and LSD test were used to analyze the p values. $p < 0.05$ was regarded as a statistically significant difference. Kaplan–Meier plots and log-rank tests were used for tumor growth inhibition tests.

3 Results

*3.1 Characterization of SA-mGM-CSF*

The protein was purified using the DEAE column, the purity of which was verified by SDS-PAGE gel electrophoresis as shown in Figs. 1A and 1B, indicating its purity as high as 97.3%. SA-mGM-CSF stimulated the bone marrow cells in a function of its dose (Fig. 1C). FCM analysis showed that the binding rate between the SA-GM-CSF protein and the biotinylated MB49 cells could reach 96.1% (Fig. 1D).

3.2 Photothermal Effect of Nanoparticles

We investigated whether CS/GO nanoparticles were effective in increasing lesion temperature upon NIR laser irradiation (0.35 W/cm^2, 15 min). In the presence of CS/GO nanoparticles, mild hyperthermia (43°C) was achieved around the mouse bladder after 15 min of NIR irradiation (Fig. 2).
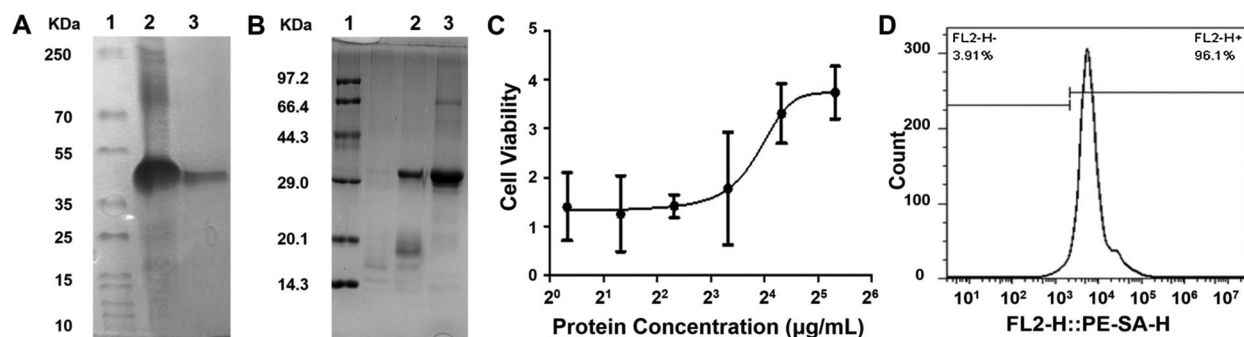
Figure 1: Characterization of SA-mGM-CSF. (A) Gel electrophoresis experiments analyzed the purification of SA-mGM-CSF fusion protein. Lane 1. Protein marker; Lane 2. Inclusion bodies of SA-GM-CSF; Lane 3. SA-mGM-CSF purified by DEAE column. (B) Analysis of the renaturation of SA-mGM-CSF fusion protein by gel electrophoresis experiments. Lane 1. Protein marker; Lane 2. Under reducing/denaturing conditions; Lane 3. Under reducing/denaturing conditions. Experiments were repeated three times. (C) Bioactivity of SA-mGM-CSF was analyzed by testing the proliferative capacity of bone marrow cells. (D) Anchoring of SA-mGM-CSF protein on the surface of biotinylated MB49 cells. Each experiment was repeated three times
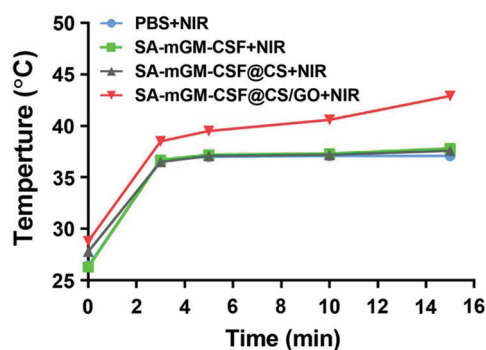
Figure 2: The temperature in the bladder region of mice was monitored by infrared thermometry. We tested the body surface temperature of mice 24 h after the successful establishment of the mouse bladder model and 30 min after the administration of the nanoparticles
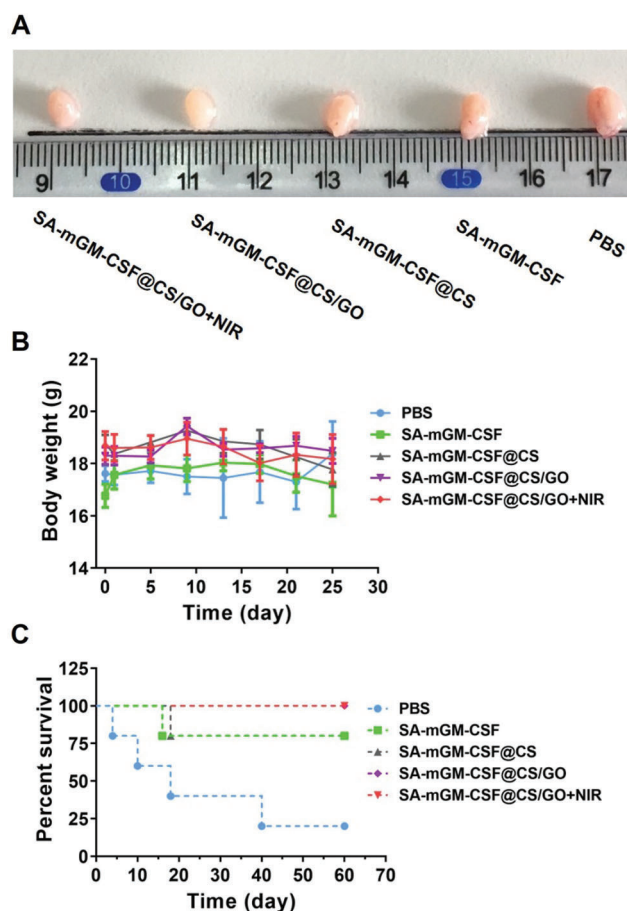
3.3 In Vivo Antitumor Effect

We further investigated the antitumor effect of CS/GO nanoparticles in an orthotopic tumor model generated from MB49 cells. As shown in Fig. 3A, SA-mGM-CSF@CS/GO plus NIR showed the best tumor suppression effect. The mean body weight of each treatment group was maintained during the treatment period. As shown in Fig. 3C, all mice in the SA-mGM-CSF@CS/GO plus NIR group survived for 60 days after the treatment.

3.4 Hematoxylin and Eosin (H&E) Staining Analysis

To investigate the inhibitory effects of different nanoparticles on bladder tumors and their effects on other important organs, we randomly sectioned and further H&E stained the bladder tissues from mice in different treatment groups after days 3, 7, and 15 of bladder cancer treatment, respectively. The results showed that the number of tumor cells in the PBS group was higher than that of other groups, and the tumor cells had a typical morphology that filled the entire bladder lumen (Fig. 4). In the other treatment groups, the numbers of tumor cells in the bladder decreased with the treatments. In particular, in the

SA-mGM-CSF@CS/GO+NIR group, many infiltrating lymphocytes also appeared under the combined effect of thermotherapy and immunotherapy, which synergistically stimulated the immune response of the bladder tumor lesions, thus killing the tumor cells.


Figure 3: Antitumor effects of different treatment groups *in vivo*. (A) Representative images of the bladder after various treatments. (B) Body weight changes of mice after treatments with different administration methods. (C) Survival rate analysis of mice in different treatment groups

The histological morphology of the heart, liver, spleen, lung, and kidney was normal in all treated groups of mice, with no significant differences between groups (Fig. 4). In contrast, the formation of lung metastases from bladder cancer was occasionally seen in the PBS group. Combined with the above H&E staining results of tumor sections, it indicates that the nanoparticles loaded with SA-mGM-CSF had no side effects during the treatment of bladder cancer and can be presumed to have the effect of preventing tumor metastasis.

3.5 Immune Responses of Different Treatments

FCM analysis delineated that the numbers of DCs (CD11c$^+$CD11b$^+$) and mature DCs (CD11c$^+$CD86$^+$) were significantly increased in the SA-mGM-CSF@CS/GO+NIR group compared with other control groups (Figs. 5B and 5C). This suggested that SA-mGM-CSF@CS/GO increased the number of DCs and the number of mature DCs. This could be attributed to the controlled release of GM-CSF by

SA-mGM-CSF@CS/GO nanoparticles. Thus, more DCs could be recruited into the bladder tumor microenvironment and facilitate subsequent antigen delivery.
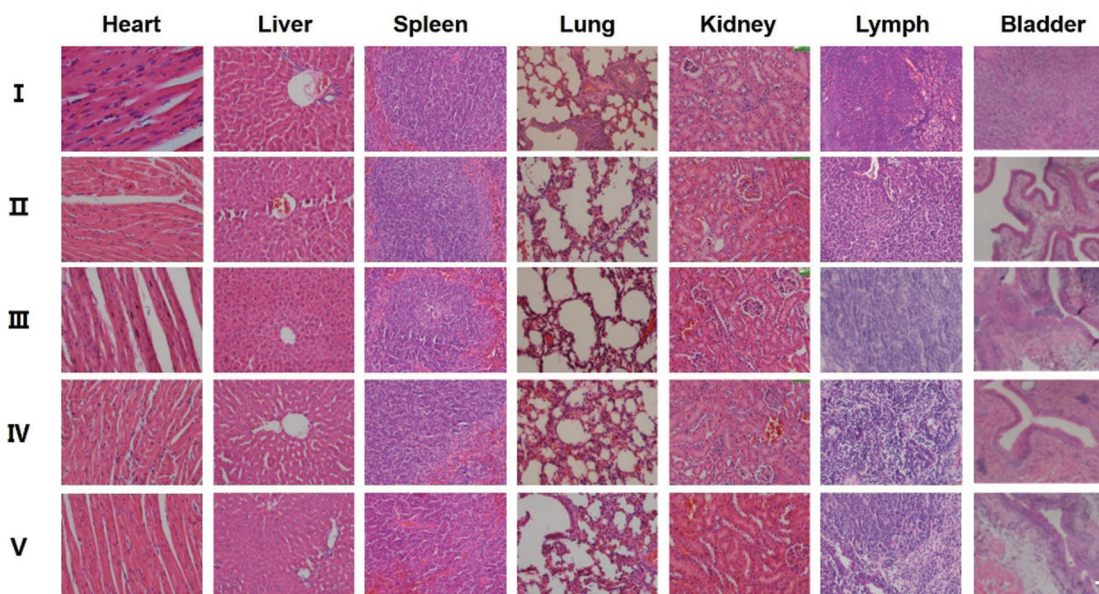
Figure 4: Representative H&E sections of tissues of different treatment groups of mice. H&E staining of mice organs and the tumor bearing murine bladder after treatment with different groups. All pictures were at a magnification of 20, Scale bar is 50 μm. (I) PBS, (II) SA-mGM-CSF, (III) SA-mGM-CSF@CS, (IV) SA-mGM-CSF@CS/GO, (V) SA-mGM-CSF@CS/GO+NIR

In general, exogenous antigens are digested in lysosomes and subsequently packed onto MHC-II to activate $CD4^+$ T cells and trigger immune responses. The endogenous antigens recognized by the MHC-I stimulates $CD8^+$ T cells and evokes cellular immunity, which is pivotal for antitumor immunotherapy. The SA-mGM-CSF@CS/GO group showed a relatively high level of $CD4^+$ T cells, as SA-mGM-CSF@CS/GO promoted more tumor-exogenous antigens into DCs. The increment of $CD4^+$ T and $CD8^+$ T lymphocytes led to an enhanced antitumor immune effect. NK cells are a particular type of monocyte and an important cytotoxic effector cell for killing tumor cells. As shown in Figs. 5B, NK cells were significantly increased in SA-mGM-CSF@CS/GO+NIR compared to the other four groups (**$p < 0.01$).

4 Discussions

Intravesical SA-mGM-CSF installation into the urinary bladder has been investigated for MB49 bladder cancer in mice. The effectiveness of the intravesical therapy relies on the retention time of the drug in the bladder. Therefore, the present study explored the feasibility and efficacy of SA-mGM-CSF@CS/GO nano-delivery system, which could be immobilized onto the biotin decorated bladder for sustained delivery of the immune adjuvant SA-mGM-CSF by the intravesical route.

The nanosystem comprises chitosan, GO, and SA-mGM-CSF, which was prepared by a nonsolvent counterion complexation method. Then a crosslinking agent of glutaraldehyde was used to enhance the structural stability of nanoparticles in the normal physiological condition. Chitosan is a positively charged, biocompatible, and biodegradable biopolymer. The positive charge and excess aldehyde groups on the surface of nanoparticles contribute to the loading of SA-mGM-CSF. GO can convert light into heat to

suppress tumor cells by its strong light absorption capacity in the near-infrared spectral region. At the same time, their photothermal effect can change the local microenvironment of the tumor, such as the permeability of blood vessels and tumor stroma, and facilitate the recruitment and migration of antigen-presenting cells such as DCs. The receptor for GM-CSF is present on the surface of a large number of cells, including DCs and macrophages. It enhances the expression of major histocompatibility complex molecules on APCs. It plays an essential role in the differentiation and maturation of DCs, which plays a key role in stimulating the antitumor immunity of T cells.
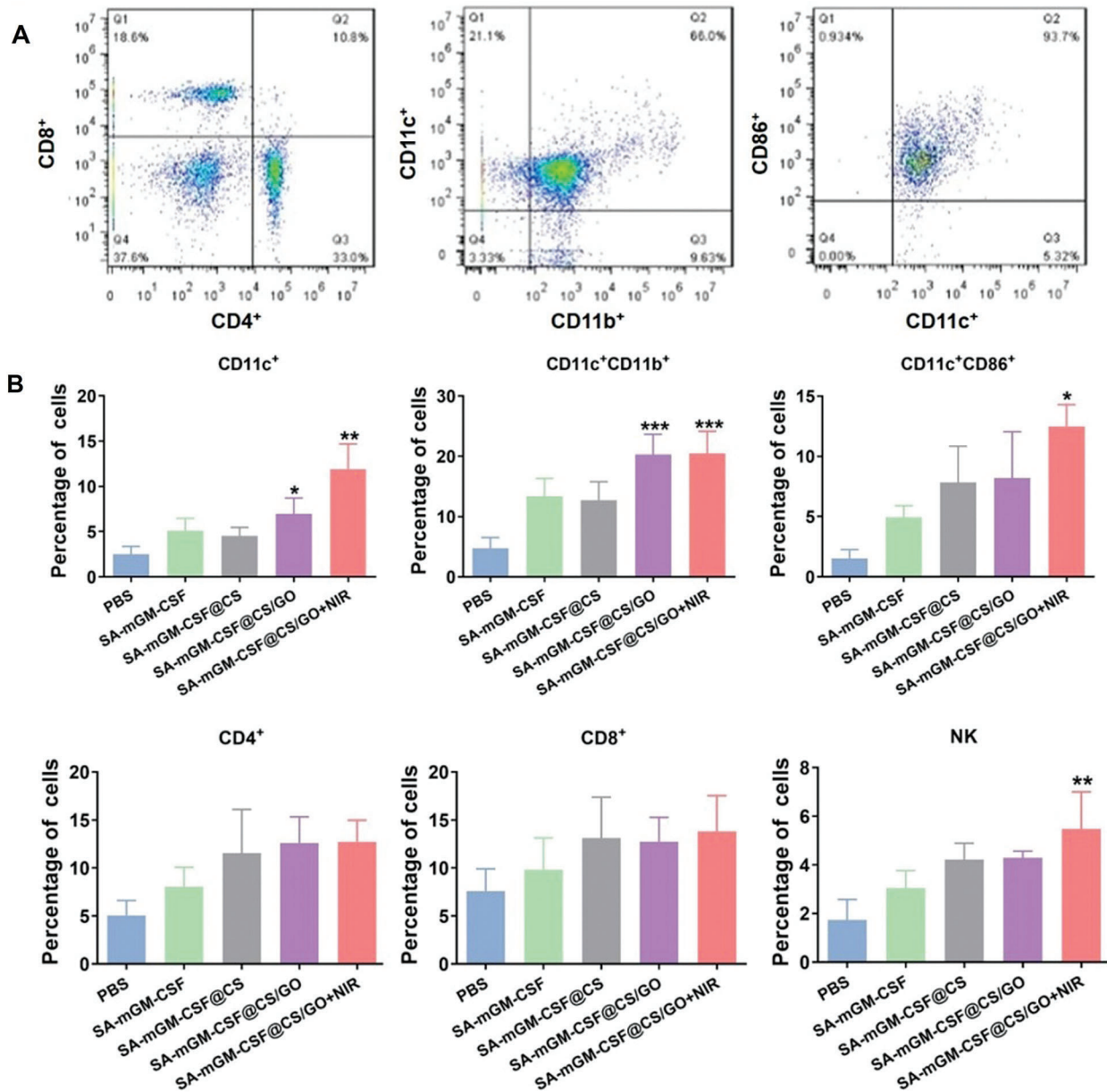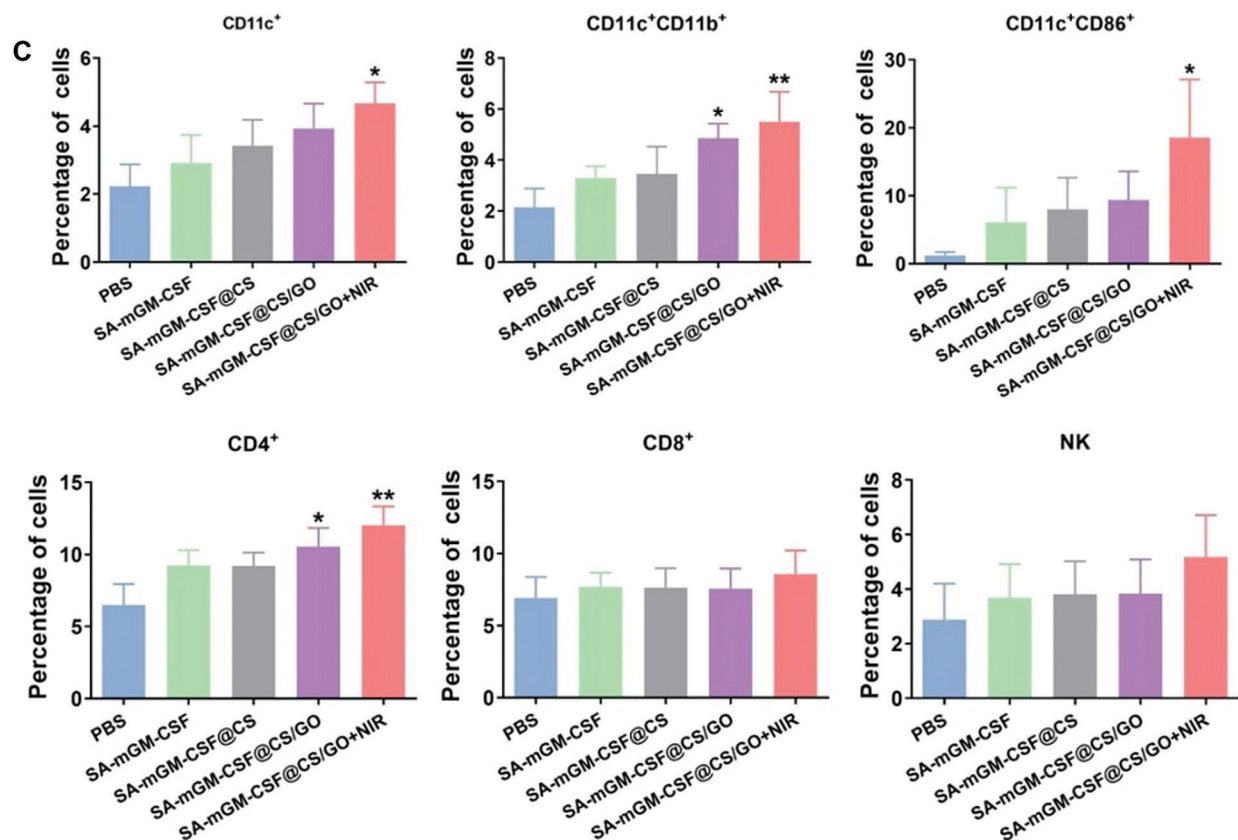

Figure 5: (continued)

Figure 5: Recruitment and activation of innate and adaptive immune cells stimulated by different groups. (A) Representative flow cytometry plots of the cells isolated from the bladder. (B) Local immune cell changes in the bladder of each treatment group after 15 days. (C) Systemic immune cell changes in peripheral blood of each treatment group after 15 days. Error bars are based on SEM (***$p < 0.001$, **$p < 0.01$, or *$p < 0.05$, by ANOVA with LSD test)

The SA-mGM-CSF@CS/GO group can rapidly increase the temperature around the bladder area upon NIR light irradiation. Typically, mild hyperthermia of approximately 43°C was detected around the mouse bladder after 15 min of NIR irradiation in the presence of CS/GO nanoparticles. After treatment by NIR light irradiation, the bladder in the nanoparticle-treated group has about one-third volume of the SA-mGM-CSF-treated group. In particular, the bladder in the SA-mGM-CSF@CS/GO+NIR group nearly returned to standard size. The results of H&E staining show that the nanoparticle treatment can inhibit the growth of bladder tumor cells and a large number of lymphocytes appeared in the SA-mGM-CSF@CS/GO group in the absence or the presence of NIR irradiation. In contrast, tumor cells in the control group proliferated significantly, even filling the entire bladder lumen and forming masses, which affected the quality of survival of the mice (~20% survival after 60 days). Most importantly, under the same conditions, mice in the SA-mGM-CSF@CS/GO nanoparticle treatment group show significant improvement in hematuria and bladder pain compared with the SA-mGM-CSF treatment group. Meanwhile, SA-mGM-CSF@CS/GO nanoparticle treatment group exhibits a higher tumor suppression rate, fewer toxic side effects, less bladder tissue lesions, and more prolonged survival. The *in vivo* therapeutic study results strongly suggest that photothermal nanoparticles combined with immunotherapy have better antitumor effects compared with SA-mGM-CSF infusion alone.

Moreover, GM-CSF could motivate mature DCs from immature cells and recruit the DCs to the local tumor microenvironment, which plays a decisive role in developing DCs in the immune response. The eventual impact of anticancer immunity rests with the action of T lymphocytes. DCs are intermediates of T lymphocytes immunity and the most effective antigen-presenting cells. In a previous study, anchoring SA-mGM-CSF on biotinylated orthotopic bladder cancer can induce specific antitumor immunity in mice and significantly increased lymphocytes infiltration [50]. Our studies show that SA-mGM-CSF entrapped by CS/GO could induce a T lymphocyte-mediated immune response, such as the increase in CD4$^+$ T cells. CD4$^+$ T cells are the main effector cells in antitumor immunity, and NK cells also are the main effector cells to target the tumor cells. In addition, CS may also contribute to the enhanced local immune response in the bladder by its mucoadhesive properties and adjuvant properties. As shown in Fig. 5, the DCs (CD11c$^+$CD11b$^+$ and CD11c$^+$CD86$^+$), T cells subpopulation (CD4$^+$) and natural killer cells (NK cells) in SA-mGM-CSF@CS/GO+NIR group have significantly increased.

5 Conclusions

In this study, we investigated the efficacy of CS/GO integrated with SA-mGM-CSF in treating orthotopic bladder cancer in mice, which enabled the slow release of antitumor immune adjuvant (SA-mGM-CSF). Focal released SA-mGM-CSF could more effectively and sustainably recruit DC cells to the bladder tumor site and enhance the function of antigen-presenting cells under the thermal effect of nanoparticles, thus boosting the immune response in mice. As a result, the activated immune response in mice thus provides better antitumor effects. Meanwhile, the combined thermal effect of SA-mGM-CSF@CS/GO nanoparticles induced a significant increase of DC cells and immune cells (T cells, etc.) in the treatment group compared with the other groups, which confirmed that the photothermal effect of nanoparticles had a positive effect on the antitumor immune response in the tumor. This strategy has been evidenced as very promising for the treatment of this specific tumor. Nevertheless, the strategy is still at its infant stage, demanding more comprehensive study, such as the large-scale preparation of nanoparticles, the control of the physicochemical property of nanoparticles, and the high-anchoring rate of nanoparticles onto the tumor area, etc.

Conflicts of Interest: The authors declare that they have no conflicts of interest to report regarding the present study.

References

1. Patel, V. G., Oh, W. K., Galsky, M. D. (2020). Treatment of muscle-invasive and advanced bladder cancer in 2020. *CA: A Cancer Journal for Clinicians, 70(5),* 404–423. DOI 10.3322/caac.21631.

2. Merchant, M. S., Bernstein, D., Amoako, M., Baird, K., Fleisher, T. A. et al. (2016). Adjuvant immunotherapy to improve outcome in high-risk pediatric sarcomas. *Clinical Cancer Research, 22(13),* 3182–3191. DOI 10.1158/1078-0432.CCR-15-2550.

3. Begley, J., Ribas, A. (2008). Targeted therapies to improve tumor immunotherapy. *Clinical Cancer Research, 14(14),* 4385–4391. DOI 10.1158/1078-0432.CCR-07-4804.

4. Min, Y., Roche, K. C., Tian, S., Eblan, M. J., McKinnon, K. P. et al. (2017). Antigen-capturing nanoparticles improve the abscopal effect and cancer immunotherapy. *Nature Nanotechnology, 12(9),* 877–882. DOI 10.1038/nnano.2017.113.

5. Feng, B., Zhou, F., Hou, B., Wang, D., Wang, T. et al. (2018). Binary cooperative prodrug nanoparticles improve immunotherapy by synergistically modulating immune tumor microenvironment. *Advanced Materials, 30(38),* 1803001. DOI 10.1002/adma.201803001.

6. Perez, C. R., de Palma, M. (2019). Engineering dendritic cell vaccines to improve cancer immunotherapy. *Nature Communications, 10(1),* 5408. DOI 10.1038/s41467-019-13368-y.

7. Huang, Y., Chen, Y., Zhou, S., Chen, L., Wang, J. et al. (2020). Dual-mechanism based CTLs infiltration enhancement initiated by nano-sapper potentiates immunotherapy against immune-excluded tumors. *Nature Communications, 11(1),* 622. DOI 10.1038/s41467-020-14425-7.

8. Wu, X., Giobbie-Hurder, A., Connolly, E. M., Li, J., Liao, X. et al. (2018). Anti-CTLA-4 based therapy elicits humoral immunity to galectin-3 in patients with metastatic melanoma. *OncoImmunology, 7(7),* e1440930. DOI 10.1080/2162402X.2018.1440930.

9. Heidenreich, R., Jasny, E., Kowalczyk, A., Lutz, J., Probst, J. et al. (2015). A novel RNA-based adjuvant combines strong immunostimulatory capacities with a favorable safety profile. *International Journal of Cancer, 137(2),* 372–384. DOI 10.1002/ijc.29402.

10. Wilson, R. M., Danishefsky, S. J. (2013). A vision for vaccines built from fully synthetic tumor-associated antigens: From the laboratory to the clinic. *Journal of the American Chemical Society, 135(39),* 14462–14472. DOI 10.1021/ja405932r.

11. Jiang, G. M., Tan, Y., Wang, H., Peng, L., Chen, H. T. et al. (2019). The relationship between autophagy and the immune system and its applications for tumor immunotherapy. *Molecular Cancer, 18(1),* 17. DOI 10.1186/s12943-019-0944-z.

12. Correale, P., Campoccia, G., Tsang, K. Y., Micheli, L., Cusi, M. G. et al. (2001). Recruitment of dendritic cells and enhanced antigen-specific immune reactivity in cancer patients treated with hr-GM-CSF (molgramostim) and hr-IL-2: Results from a phase Ib clinical trial. *European Journal of Cancer, 37(7),* 892–902. DOI 10.1016/S0959-8049(01)00063-6.

13. Pardoll, D. M. (2012). The blockade of immune checkpoints in cancer immunotherapy. *Nature Reviews Cancer, 12(4),* 252–264. DOI 10.1038/nrc3239.

14. Mellman, I., Coukos, G., Dranoff, G. (2011). Cancer immunotherapy comes of age. *Nature, 480(7378),* 480–489. DOI 10.1038/nature10673.

15. Zhang, X., Mozeleski, B., Lemoine, S., Dériaud, E., Lim, A. et al. (2014). CD4 T cells with effector memory phenotype and function develop in the sterile environment of the fetus. *Science Translational Medicine, 6(238),* 238ra272. DOI 10.1126/scitranslmed.3008748.

16. van Tendeloo, V. F. I., van Broeckhoven, C., Berneman, Z. N. (2001). Gene-based cancer vaccines: An *ex vivo* approach. *Leukemia, 15(4),* 545–558. DOI 10.1038/sj.leu.2402069.

17. Zou, L., Wang, H., He, B., Zeng, L., Tan, T. et al. (2016). Current approaches of photothermal therapy in treating cancer metastasis with nanotherapeutics. *Theranostics, 6(6),* 762–772. DOI 10.7150/thno.14988.

18. Huang, T., Zhao, M., Yu, Q., Feng, Z., Xie, M. et al. (2019). De novo design of polymeric carrier to photothermally release singlet oxygen for hypoxic tumor treatment. *Research, 2019,* 1–11. DOI 10.34133/2019/9269081.

19. Dai, H., Shen, Q., Shao, J., Wang, W., Gao, F. et al. (2021). Small molecular NIR-II fluorophores for cancer phototheranostics. *The Innovation, 2(1),* 100082. DOI 10.1016/j.xinn.2021.100082.

20. Bi, Y., Wang, M., Peng, L., Ruan, L., Zhou, M. et al. (2020). Photo/thermo-responsive and size-switchable nanoparticles for chemo-photothermal therapy against orthotopic breast cancer. *Nanoscale Advances, 2(1),* 210–213. DOI 10.1039/C9NA00652D.

21. Gao, H., Bi, Y., Chen, J., Peng, L., Wen, K. et al. (2016). Near-infrared light-triggered switchable nanoparticles for targeted chemo/photothermal cancer therapy. *ACS Applied Materials & Interfaces, 8(24),* 15103–15112. DOI 10.1021/acsami.6b03905.

22. Gao, H., Bi, Y., Wang, X., Wang, M., Zhou, M. et al. (2017). Near-infrared guided thermal-responsive nanomedicine against orthotopic superficial bladder cancer. *ACS Biomaterials Science & Engineering, 3(12),* 3628–3634. DOI 10.1021/acsbiomaterials.7b00405.

23. Qin, Y., Chen, J., Bi, Y., Xu, X., Zhou, H. et al. (2015). Near-infrared light remote-controlled intracellular anti-cancer drug delivery using thermo/pH sensitive nanovehicle. *Acta Biomaterialia, 17,* 201–209. DOI 10.1016/j.actbio.2015.01.026.

24. Wen, K., Zhou, M., Lu, H., Bi, Y., Ruan, L. et al. (2018). Near-infrared/pH dual-sensitive nanocarriers for enhanced intracellular delivery of doxorubicin. *ACS Biomaterials Science & Engineering, 4(12),* 4244–4254. DOI 10.1021/acsbiomaterials.8b01051.

25. Wang, D., Zhou, M., Huang, H., Ruan, L., Lu, H. et al. (2019). Gold nanoparticle-based probe for analyzing mitochondrial temperature in living cells. *ACS Applied Bio Materials, 2(8),* 3178–3182. DOI 10.1021/acsabm.9b00463.

26. Dreaden, E. C., Alkilany, A. M., Huang, X., Murphy, C. J., El-Sayed, M. A. (2012). The golden age: Gold nanoparticles for biomedicine. *Chemical Society Reviews, 41(7),* 2740–2779. DOI 10.1039/C1CS15237H.

27. Zhu, H., Chen, Y., Yan, F. J., Chen, J., Tao, X. F. et al. (2017). Polysarcosine brush stabilized gold nanorods for *in vivo* near-infrared photothermal tumor therapy. *Acta Biomaterialia, 50(11),* 534–545. DOI 10.1016/j.actbio.2016.12.050.

28. Liu, Y., Li, H., Xie, J., Zhou, M., Huang, H. et al. (2017). Facile construction of mitochondria-targeting nanoparticles for enhanced phototherapeutic effects. *Biomaterials Science, 5(5),* 1022–1031. DOI 10.1039/C6BM00878J.

29. Yang, K., Feng, L., Shi, X., Liu, Z. (2013). Nano-graphene in biomedicine: Theranostic applications. *Chemical Society Reviews, 42(2),* 530–547. DOI 10.1039/C2CS35342C.

30. Lima-Sousa, R., de Melo-Diogo, D., Alves, C. G., Costa, E. C., Ferreira, P. et al. (2018). Hyaluronic acid functionalized green reduced graphene oxide for targeted cancer photothermal therapy. *Carbohydrate Polymers, 200(27),* 93–99. DOI 10.1016/j.carbpol.2018.07.066.

31. Yin, F., Hu, K., Chen, Y., Yu, M., Wang, D. et al. (2017). siRNA delivery with pegylated graphene oxide nanosheets for combined photothermal and genetherapy for pancreatic cancer. *Theranostics, 7(5),* 1133–1148. DOI 10.7150/thno.17841.

32. Liu, Y., Holder, T., Yan, B. (2021). Chirality-induced giant unidirectional magnetoresistance in twisted bilayer graphene. *The Innovation, 2(1),* 100085. DOI 10.1016/j.xinn.2021.100085.

33. Wang, J., Chang, Y., Luo, H., Jiang, W., Xu, L. et al. (2020). Designing immunogenic nanotherapeutics for photothermal-triggered immunotherapy involving reprogramming immunosuppression and activating systemic antitumor responses. *Biomaterials, 255,* 120153. DOI 10.1016/j.biomaterials.2020.120153.

34. Ruan, L., Wang, M., Zhou, M., Lu, H., Zhang, J. et al. (2019). Doxorubicin-metal coordinated micellar nanoparticles for intracellular codelivery and chemo/chemodynamic therapy *in vitro*. *ACS Applied Bio Materials, 2(11),* 4703–4707. DOI 10.1021/acsabm.9b00879.

35. Ruan, L., Zhou, M., Chen, J., Huang, H., Zhang, J. et al. (2019). Thermoresponsive drug delivery to mitochondria *in vivo*. *Chemical Communications, 55(97),* 14645–14648. DOI 10.1039/C9CC07538K.

36. Wang, D., Huang, H., Zhou, M., Lu, H., Chen, J. et al. (2019). A thermoresponsive nanocarrier for mitochondria-targeted drug delivery. *Chemical Communications, 55(28),* 4051–4054. DOI 10.1039/C9CC00603F.

37. Zhou, M., Wen, K., Bi, Y., Lu, H., Chen, J. et al. (2017). The application of stimuli-responsive nanocarriers for targeted drug delivery. *Current Topics in Medicinal Chemistry, 17(20),* 2319–2334. DOI 10.2174/1568026617666170224121008.

38. Zhou, M., Zhang, X., Xie, J., Qi, R., Lu, H. et al. (2018). pH-sensitive poly(β-amino ester)s nanocarriers facilitate the inhibition of drug resistance in breast cancer cells. *Nanomaterials, 8(11),* 952. DOI 10.3390/nano8110952.

39. Du, J., Lane, L. A., Nie, S. (2015). Stimuli-responsive nanoparticles for targeting the tumor microenvironment. *Journal of Controlled Release, 219,* 205–214. DOI 10.1016/j.jconrel.2015.08.050.

40. Chen, Q., Hu, Q., Dukhovlinova, E., Chen, G., Ahn, S. et al. (2019). Photothermal therapy promotes tumor infiltration and antitumor activity of Car T cells. *Advanced Materials, 31(23),* 1900192. DOI 10.1002/adma.201900192.

41. Wang, P., Zhang, H., Cui, Z., Jin, X., Zhang, D. (2021). Mir-612 inhibits proliferation and invasion of urothelial carcinoma of bladder cells through activating hippo pathway via targeting PMEPA1. *Oncologie, 23(2),* 259–268. DOI 10.32604/Oncologie.2021.015503.

42. Hong, I. S. (2016). Stimulatory versus suppressive effects of GM-CSF on tumor progression in multiple cancer types. *Experimental & Molecular Medicine, 48(7),* e242. DOI 10.1038/emm.2016.64.

43. Zhang, X., Shi, X., Li, J., Hu, Z., Zhou, D. et al. (2012). A novel therapeutic vaccine of mouse GM-CSF surface modified MB49 cells against metastatic bladder cancer. *The Journal of Urology, 187(3),* 1071–1079. DOI 10.1016/j.juro.2011.10.126.

44. Arai, S., Suzuki, M., Park, S. J., Yoo, J. S., Wang, L. et al. (2015). Mitochondria-targeted fluorescent thermometer monitors intracellular temperature gradient. *Chemical Communications, 51(38),* 8044–8047. DOI 10.1039/C5CC01088H.

45. Du, C., Zhou, M., Jia, F., Ruan, L., Lu, H. et al. (2021). D-arginine-loaded metal-organic frameworks nanoparticles sensitize osteosarcoma to radiotherapy. *Biomaterials, 269,* 120642. DOI 10.1016/j.biomaterials.2020.120642.

46. Geng, H., Zhou, M., Li, B., Liu, L., Yang, X. et al. (2021). Metal-drug nanoparticles-mediated osteolytic microenvironment regulation for enhanced radiotherapy of orthotopic osteosarcoma. *Chemical Engineering Journal, 417(1),* 128103. DOI 10.1016/j.cej.2020.128103.

47. Huang, H., Zhou, M., Ruan, L., Wang, D., Lu, H. et al. (2019). AMPK mediates the neurotoxicity of iron oxide nanoparticles retained in mitochondria or lysosomes. *Metallomics, 11(7),* 1200–1206. DOI 10.1039/C9MT00103D.

48. Chen, J., Shi, M., Liu, P., Ko, A., Zhong, W. et al. (2014). Reducible polyamidoamine-magnetic iron oxide self-assembled nanoparticles for doxorubicin delivery. *Biomaterials, 35(4),* 1240–1248. DOI 10.1016/j.biomaterials.2013.10.057.

49. Zhou, M., Huang, H., Wang, D., Lu, H., Chen, J. et al. (2019). Light-triggered PEGylation/dePEGylation of the nanocarriers for enhanced tumor penetration. *Nano Letters, 19(6),* 3671–3675. DOI 10.1021/acs.nanolett.9b00737.

50. Hu, Z., Tan, W., Zhang, L., Liang, Z., Xu, C. et al. (2010). A novel immunotherapy for superficial bladder cancer by intravesical immobilization of GM-CSF. *Journal of Cellular and Molecular Medicine, 14(6b),* 1836–1844. DOI 10.1111/j.1582-4934.2009.00818.x.